Polarization state studies in second harmonic generation signals to trace atherosclerosis lesions

Camille Doras,[1,4] Gregory Taupier,[2] Alberto Barsella,[2] Loïc Mager,[2] Alex Boeglin,[2] Hervé Bulou,[2] Pascal Bousquet,[1] and Kokou D. Dorkenoo[2,3]

[1]LNPCV EA 4438, Faculté de médecine, 11 rue Humann, 67 000 Strasbourg, France
[2]IPCMS UMR 7504, 23 rue du Loess, France
[3]dorkenoo@ipcms.ustrasbg.fr
[4]camille.doras@unistra.fr

Abstract: We have performed multi-photon image reconstructions as well as polarization state analyses inside an artery wall affected by atherosclerosis to investigate the changes in collagen structure. Mice, either healthy or affected by spontaneous atherosclerosis, have been used for this purpose. A two-photon imaging system has been used to investigate atherosclerotic lesions in the ascending aorta of mice. Second harmonic imaging has been performed alternatively on healthy samples and on affected region. The reconstructed images show that the spatial distribution of the collagen network seems disorganized by the disease. The polarization state studies reveal however that the apparent disorganization of the collagen is related to its spatially diffuse distribution and that the internal structure of the collagen fibers is not affected by the disease. In addition, a theoretical simulation of the second harmonic polarization states shows that they are consistent with the known 3D structure of the collagen network.

OCIS codes: (180.4315) Nonlinear microscopy; (190.1900) Diagnostic applications of nonlinear optics.

References and links

1. S. Roth and I. Freund, "Second-harmonic generation in collagen," J. Chem. Phys. **70**(4), 1637–1643 (1979).
2. P. J. Campagnola, A. C. Millard, M. Terasaki, P. E. Hoppe, C. J. Malone, and W. A. Mohler, "Three-dimensional high-resolution second-harmonic generation imaging of endogenous structural proteins in biological tissues," Biophys. J. **82**(1), 493–508 (2002).
3. R. M. Williams, W. R. Zipfel, and W. W. Webb, "Interpreting second-harmonic generation images of collagen I fibrils," Biophys. J. **88**(2), 1377–1386 (2005).
4. M. Strupler, A. M. Pena, M. Hernest, P. L. Tharaux, J. L. Martin, E. Beaurepaire, and M. C. Schanne-Klein, "Second harmonic imaging and scoring of collagen in fibrotic tissues," Opt. Express **15**(7), 4054–4065 (2007).
5. W. R. Zipfel, R. M. Williams, R. Christie, A. Y. Nikitin, B. T. Hyman, and W. W. Webb, "Live tissue intrinsic emission microscopy using multiphoton-excited native fluorescence and second harmonic generation," Proc. Natl. Acad. Sci. U.S.A. **100**(12), 7075–7080 (2003).
6. S. W. Chu, S. P. Tai, M. C. Chan, C. K. Sun, I. C. Hsiao, C. H. Lin, Y. C. Chen, and B. L. Lin, "Thickness dependence of optical second harmonic generation in collagen fibrils," Opt. Express **15**(19), 12005–12010 (2007).
7. S. Brasselet, D. Ait-Belkacem, A. Gasecka, F. Munhoz, S. Brustlein, and S. Brasselet, "Influence of birefringence on polarization resolved nonlinear microscopy and collagen SHG structural imaging," Opt. Express **18**(14), 14859–14870 (2010).
8. I. Gusachenko, G. Latour, and M. C. Schanne-Klein, "Polarization-resolved Second Harmonic microscopy in anisotropic thick tissues," Opt. Express **18**(18), 19339–19352 (2010).
9. P. J. Su, W. L. Chen, J. B. Hong, T. H. Li, R. J. Wu, C. K. Chou, S. J. Chen, C. Hu, S. J. Lin, and C. Y. Dong, "Discrimination of collagen in normal and pathological skin dermis through second-order susceptibility microscopy," Opt. Express **17**(13), 11161–11171 (2009).
10. A. Zoumi, X. Lu, G. S. Kassab, and B. J. Tromberg, "Imaging coronary artery microstructure using second-harmonic and two-photon fluorescence microscopy," Biophys. J. **87**(4), 2778–2786 (2004).
11. T. Boulesteix, A. M. Pena, N. Pages, G. Godeau, M. P. Sauviat, E. Beaurepaire, and M. C. Schanne-Klein, "Micrometer scale ex vivo multiphoton imaging of unstained arterial wall structure," Cytometry A **69**(1), 20–26 (2006).

#145350 - $15.00 USD Received 4 Apr 2011; revised 30 Jun 2011; accepted 30 Jun 2011; published 21 Jul 2011

12. T. T. Le, I. M. Langohr, M. J. Locker, M. Sturek, and J. X. Cheng, "Label-free molecular imaging of atherosclerotic lesions using multimodal nonlinear optical microscopy," J. Biomed. Opt. **12**(5), 054007 (2007).
13. H. W. Wang, I. M. Langohr, M. Sturek, and J. X. Cheng, "Imaging and quantitative analysis of atherosclerotic lesions by CARS-based multimodal nonlinear optical microscopy," Arterioscler. Thromb. Vasc. Biol. **29**(9), 1342–1348 (2009).
14. R. S. Lim, A. Kratzer, N. P. Barry, S. Miyazaki-Anzai, M. Miyazaki, W. W. Mantulin, M. Levi, E. O. Potma, and B. J. Tromberg, "Multimodal CARS microscopy determination of the impact of diet on macrophage infiltration and lipid accumulation on plaque formation in ApoE-deficient mice," J. Lipid Res. **51**(7), 1729–1737 (2010).
15. P. A. Franken, A. E. Hill, C. W. Peters, and G. W. Weinreich, "Generation of optical harmonics," Phys. Rev. Lett. **7**(4), 118–119 (1961).
16. D. A. Kleinman, "Theory of second harmonic generation of light," Phys. Rev. **128**(4), 1761–1775 (1962).
17. S. Roth and I. Freund, "Second harmonic generation and orientational order in connective tissue: a mosaic model for fibril orientational ordering in rat-tail tendon," J. Appl. Cryst. **15**(1), 72–78 (1982).
18. I. Freund, M. Deutsch, and A. Sprecher, "Connective tissue polarity. Optical second-harmonic microscopy, crossed-beam summation, and small-angle scattering in rat-tail tendon," Biophys. J. **50**(4), 693–712 (1986).

1. Introduction

It is widely known that collagen, the most important structural protein of the animal body, is a well-structured non-centrosymmetric medium. Its unique triple-helix structure and extremely high level of crystallinity make it exceptionally efficient in the generation of the second harmonic from incident light [1]. As a result, second harmonic generation (SHG) microscopy of collagen produces strong and robust signals, providing an invaluable tool for imaging biological tissue with submicron resolution [2–4].

In recent years, many SHG experiments have been devoted to the study of collagen structures in biological tissues [5]. For example, Chu and associates have used SHG microscopy to determine collagen thicknesses [6] while Brassellet et al. have used the same setup to determine the influence of birefringence on image reconstruction using rat tail tendon collagen [7,8]. A possible medical application has been proposed by Su et al. which have used SHG imaging as a quantitative method for diagnosing dermal pathology [9]. Several authors used SHG and two photon excitation fluorescence (TPEF) to distinguish collagen from elastin fibers in artery walls [5,10,11]. Fibrillar collagen is also a well-known element involved in the formation of atherosclerotic lesions. In an Ossabow pig model, Le et al. and Wang et al. exploited multimodal non-linear optical applications to image atherosclerosis structure and stages [12,13]. Finally, Lim et al. applied non-linear systems to detect atherosclerosis in C57BL6 and ApoE knockout mice [14].

In this letter, we have used SHG polarization resolved imaging to study the evolution of the collagen structure in atherosclerosis. Indeed, the changes in spatial coherence of collagen may provide valuable information about the damages caused by the disease. In particular, high resolution information, such as provided by the SHG process, will prove important in characterizing the state of the collagen structure during the disease evolution.

2. Specimen and Sample Preparation

All animal care procedures were performed in accordance with the *Comité Régional d'Ethique en matière d'expérimentation animale of Strasbourg*. Forty week-old C57BL/6 mice, bred within our husbandry and 28 week-old apolipoprotein E knockout ($ApoE^{-/-}$) mice on a C57BL/6 background purchased from Taconic (Ejby, Denmark) were used. $ApoE^{-/-}$ mice develop spontaneous atherosclerosis lesions and are known to be one of the gold standards of atherosclerosis animal models. Animals were housed within the medicine faculty facilities, exposed to a 12-hours light / 12-hours dark cycle and maintained on a standard chow. Mice were anesthetized with an intraperitoneal injection of pentobarbital. The heart and vascular tree were perfused at 37°C under a pressure of 120 cm of water with PBS via a cannula placed in the left ventricle. The heart and the aorta were harvested and kept into neutral-buffered formalin until further process. Only ascending aortas were embedded in OCT (Tissue-Tek), and snap frozen into isopentane cooled by liquid nitrogen. Ten micrometers cross cryosections were made. Sections were fixed, dried, mounted on superfrost slides and coverslipped with

#145350 - $15.00 USD Received 4 Apr 2011; revised 30 Jun 2011; accepted 30 Jun 2011; published 21 Jul 2011

SafeMount (Labonord). Sections are not labeled. Finally, sections are submitted to Two Photon Laser Scanning Microscope observation.

3. Experimental Setup

The experimental setup is based on a confocal microscope (see Fig. 1(a)). The illumination is provided by a Spectra Physics Ti:Sapphire laser (Millenium-Tsunami combination) generating ~100 fs pulses with a repetition-rate of 80 MHz and a wavelength in the 700–1000 nm range. The scanning was performed by a motorized *XYZ* sample stage. This system is interfaced with an Olympus IX71 inverted microscope. The polarized state of the incident beam is adjusted with a half-plate placed on a motorized stage. The backscattered signal is collected in epi-mode with a dichroic mirror placed directly after the objective back aperture. This output intensity is collected by a photomultiplier. The signal is recorded as a function of the rotation angle of a Glan-analyzer placed on a motorized stage. When necessary, a filter (BG18) is placed in front of the photomultiplier to collect only the SHG signal. In all these experiments, the focusing objective consists of a Zeiss 60 × 1.3 numerical aperture (N.A.) and the illumination wavelength is centered at 800 nm.

As shown in Fig. 1(b), the output signal, sent directly to a spectrometer, consists of two parts: a very narrow peak at 400 nm which corresponds to the SHG signal and a broad band which spans fluorescence induces by two-photon absorption.

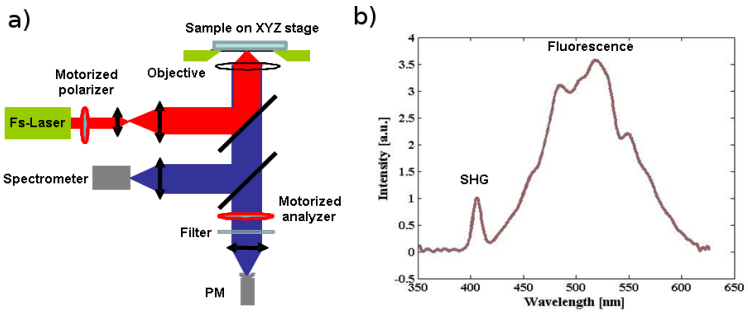

Fig. 1. Schematic drawing of the experimental setup (left) and representative spectrum recorded at the spectrometer (right).

4. Experiments on Healthy Mice

The first set of experiments was performed on samples from healthy C57BL/6 mice. The samples were prepared on microscope glass slides, as described above, and were then placed on the cell holder above the inverted microscope setup, as shown in Fig. 1.

The images reconstructed after scanning a sample are shown in Fig. 2. Figure 2(a) results from all the light collected by the photomultiplier, mainly intrinsic TPEF form elastin, while Fig. 2(b) consists in the collagen SHG signal only. Notice the difference between these two images. It is highlighted in the superposition of both pictures as displayed in Fig. 2(c) and 3(a). Figure 3(a) clearly reveals that collagen is adjacent to elastin in the media and prevalent in the adventice.

#145350 - $15.00 USD Received 4 Apr 2011; revised 30 Jun 2011; accepted 30 Jun 2011; published 21 Jul 2011

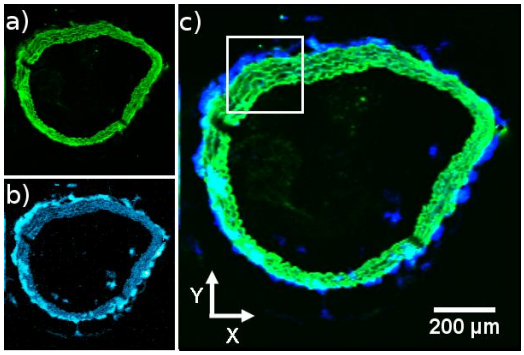

Fig. 2. TPEF and SHG cross sectional images of healthy ascending aorta from C57BL/6 mouse. (a) All 2 photon autofluorescence collected, mainly arising from elastin elastic fiber (green). (b) SHG only, specific from collagen fibers (blue). (c) Merge: TPEF and SHG signals do not overlap. (P=60 mW, Obj. x60 oil, 1,1mm x 1,1mm, step 5µm, integration time 20ms).

To avoid any artifacts caused by birefringence, we have performed the polarization state studies on the fluorescence signal only, Fig. 3(b) displays the polarization state of the fluorescence signal when the input beam is polarized at 0° (parallel to the x-axis). Each data point represented by a cross corresponds to the average intensity coming out of about a 25x25 μm^2 portion of the media. The shape of the curve is in excellent agreement with the one obtained by Shanne–Klein group [4].

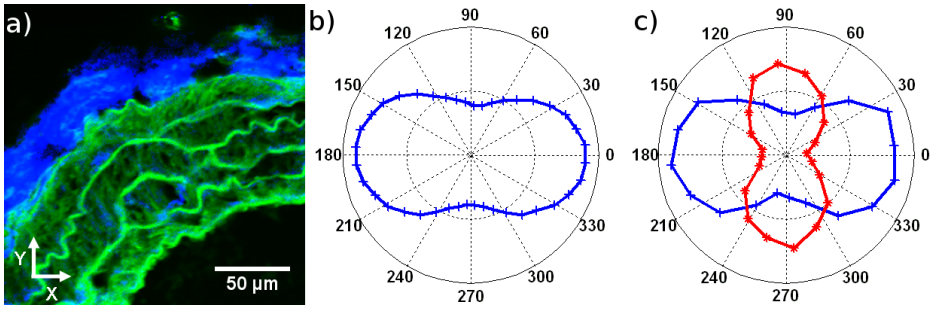

Fig. 3. Healthy C57BL:6 mouse: polarization dependence. (a) Enlarged composite image of Fig. 2. (c) ; notice the localization of collagen, adjacent to elastin in the media and prevalent in the adventice. (P=60 mW, Obj. x60 oil, 200µm x 200µm, integration time 20ms). (b) Polar diagram of the polarization state of the fluorescence. (c) Polarization state of the SHG signal (see text). (For (b) and (c) diagram from selected area in picture 25µm x 25µm, step 1µm, integration time 100 ms).

Finally, in Fig. 3(c) we present the polarization states of the SHG signal, arising from the same 25x25 μm^2 portion of the aortic media, for two positions of the entrance polarizer, once along the x-axis, displayed in blue, and once along the y-axis, displayed in red.

5. Experiments on Atherosclerotic Mice

In order to follow the evolution of the disease, the same set of experiments has also been performed on the affected $ApoE^{-/-}$ mice. In accordance with Fig. 3, Fig. 4 shows the image of same aortic part of the mouse. These two-photon images show that the section of the aorta is changed by the presence of a prominence inside the vessel lumen signaling atherosclerosis. Like in healthy aorta, the SHG signal is localized along elastic fibers in the media and in the adventice but also inside the lesion (white arrow on Fig. 5(a)).

#145350 - $15.00 USD Received 4 Apr 2011; revised 30 Jun 2011; accepted 30 Jun 2011; published 21 Jul 2011

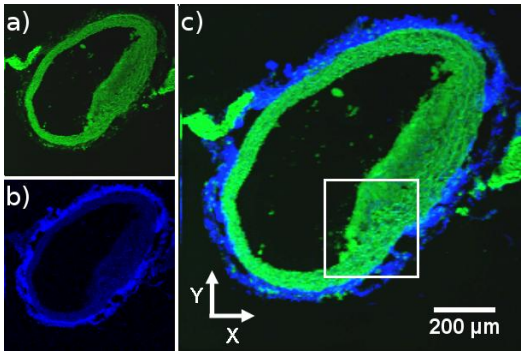

Fig. 4. TPEF and SHG cross sectional images of atherosclerotic ascending aorta from ApoE$^{-/-}$ mouse. (a) All 2 photon autofluorescence collected (green). (b) SHG only (blue). (c) Merge: TPEF and SHG signals do not overlap; the atherosclerotic plaque clearly appears as a protrusion inside the lumen. (P=60 mW, Obj. x60 oil, integration time 20ms).

Therefore, polarization states studies of the SHG signal were performed in two different regions each about 25x25 µm^2 of the affected vessel, as indicated in Fig. 5(a)). Areas 1 and 2 correspond to the region of the atherosclerotic plaque core and of the underlying media respectively. The corresponding polarization curves are represented in Fig. 5(b) and 5(c). In the media of affected ApoE$^{-/-}$ mice (Fig. 5(c)), the curves indicate that the polarization states of SHG signals are not as clearly defined as in the media of healthy C57BL/6 mice (Fig. 3(c)). For information the study of the polarization state in the region 1 (core of atherosclerotic plaque) gives an undefined polarization curves (Fig. 5(b)).

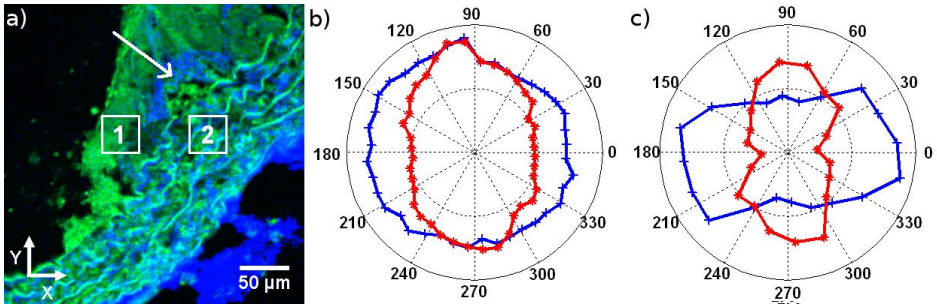

Fig. 5. Atherosclerotic ApoE$^{-/-}$ mouse: polarization dependence. (a) Enlarged composite image of Fig. 4. (c) in the atherosclerotic plaque shoulder region. Notice disruptions of the internal elastic lamina and that collagen also localizes within the plaque matrix (white arrow). (P=60 mW, Obj. x60 oil, integration time 20ms). (b) Curve of the polarization state of SHG coming from the atherosclerotic plaque (zone 1). (c) Curve of the polarization state of SHG coming from the media underlying the plaque (zone 2). (For (b) and (c) diagram from selected area in picture 25µm x 25µm, integration time 100 ms).

Comparing the two sets of the experiments one may deduce that disease has disorganized the structure of the collagen.

We have performed the same experiments by lowering the size of the studied regions to 10x10 µm^2 to select accurately collagen fibers only, for both healthy and unhealthy vessels. By keeping all other conditions equivalent to Fig. 2(b), 4(b) and Fig. 3(c), 5(c), we obtained the curves displayed in Fig. 6. Figure 6(a) and 6(b) show that healthy and atherosclerotic mice exhibit the same behavior. This behavior was observed whatever the collagen fibers from the same sample throughout the medial concentric elastic fibers (*xy* variations) or throughout the sample depth (*z* variations). It was also observed on the same selected elastic fiber (the most medial) of different mice samples (*n=6* for wild type or affected mice respectively).

#145350 - $15.00 USD Received 4 Apr 2011; revised 30 Jun 2011; accepted 30 Jun 2011; published 21 Jul 2011

Our findings show that atherosclerosis affects the superstructure of collagen fibers in the media, but that the internal structure of the fibers remains unchanged in an optical point of view.

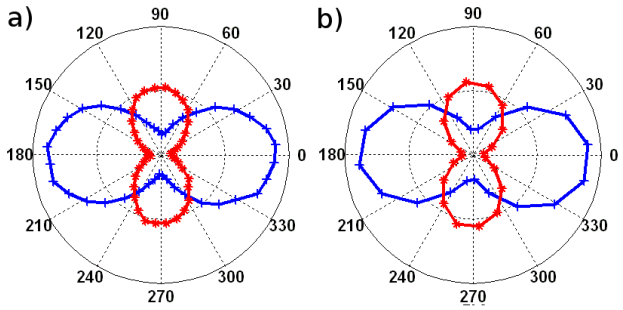

Fig. 6. Polarization states of the SHG signal precisely coming from collagen fibers of the aortic media in (a) healthy C57BL/6 and (b) atherosclerotic ApoE$^{-/-}$ mice. Healthy and atherosclerotic mice exhibit the same behavior. (For (a) and (b) diagram from selected area in picture P=30mW, 10µm x 10µm, integration time 100 ms).

6. Theoretical Explanation of the Collagen SHG Signal

Having evidenced the unchanged internal structure of the collagen fibers in both healthy and affected mice aorta, the question is now to understand the origin of the depolarization effect. We propose that it is related to spatial fiber disorganization.

In order to prove such a hypothesis, the measured SHG data were compared with calculated one. SHG, observed for acentric media, results from the radiation of a polarization including contribution $p_i^{(2)}$ oscillating at twice the incident laser radiation E frequency [15,16]:

$$p_i^{(2)} = \sum_{j=1}^{3} \sum_{k=1}^{3} \beta_{ijk} E_j E_k .$$

where β is the hyperpolarizability tensor and i, j and k refer to an orthogonal coordinate system.

In the case of collagen fibrils aligned along the *y-axis*, and for a propagation of the incident laser radiation along the *z-axis*, the radiated second-order polarization is given by [17,18]

$$P_y^{(2)} = \rho E_y^{(2)} + E_x^{(2)},$$

$$P_x^{(2)} = 2E_y E_x,$$

with

$$\rho = \frac{\beta_{yyy}}{\beta_{yxx}}.$$

For an angle α between the plane-polarized incident laser radiation aligned along the *y-axis* and the collagen fibril alignment axis, the second harmonic intensities $I_x^2(\alpha)$ and $I_y^2(\alpha)$ are given by [17,18].

In the present experiment, we sent a plane-polarized incident laser radiation for various angles α relative to the *z-axis* and we measured the second harmonic intensity $I_y^{(2)}(\alpha)$ through a polarizer oriented parallel to the *y-axis:*

#145350 - $15.00 USD Received 4 Apr 2011; revised 30 Jun 2011; accepted 30 Jun 2011; published 21 Jul 2011

$$I_x^2(\alpha) = \left(\sin(2\alpha)\right)^2,$$

$$I_y^{(2)}(\alpha) = \left(\rho\cos^2(\alpha) + \sin^2(\alpha)\right)^2.$$

In order to fit the measured polarization state of the SHG signal coming from collagen fibers of the aortic media (Fig. 6), and for taking into account the fiber disorganization, we used the above equations to calculate the total SHG signal by summing SHG contributions resulting from a Gaussian distribution of the collagen fibril alignment axis relatively to the polarization axis of incident radiation.

Figure 7 displays a comparison between measured and calculated polar plots for polarization of the incident radiation along the *y-axis* and the *x-axis*. We determined a full width at half maximum of 16.5° for the Gaussian distribution of the fiber disorientation angle α. A ratio ρ=2.5 was used to fit the measured data with the calculated one. The latter is larger than some previous reported values [17,18] but in agreement with the value 2.6 ± 0.2 recently reported by Williams et al. [5] for individual fibril.

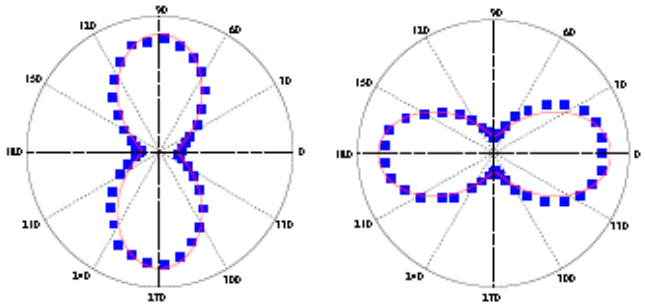

Fig. 7. Measured (blue squares) and calculated (red line) polar plots of polarization state of the SHG signal coming from collagen fibers of the aortic media (healthy) for polarization of the incident radiation along (a) the y-axis and (b) the x-axis.

7. Conclusion

In summary, we have studied the evolution of aorta affected by atherosclerosis through a nonlinear image reconstruction system combined with polarization state detection. Comparing the nonlinear optical properties of histological preparations from both healthy and affected mice aortas, we have shown that this disease brings about a structural damage reflected in the spatial coherence of the collagen. However, very high resolution images reveal that the internal structure of the triple-helix of collagen is not affect. Our interpretation of the results is justified by simple theoretical considerations. Our findings contradict therefore the conclusions drawn from previous studies that the observed depolarization was linked to collagen denaturation. Instead, we conclude that it is merely the spatial distribution of collagen in the tissue that becomes disordered.

#145350 - $15.00 USD Received 4 Apr 2011; revised 30 Jun 2011; accepted 30 Jun 2011; published 21 Jul 2011